Cancer Chemother Pharmacol (2010) 65:1145–1152
DOI 10.1007/s00280-009-1123-5

ORIGINAL ARTICLE

Pharmacokinetics and distribution of SN 28049, a novel DNA binding anticancer agent, in mice

Pradeep B. Lukka · James W. Paxton · Philip Kestell · Bruce C. Baguley

Received: 3 July 2009 / Accepted: 2 September 2009 / Published online: 23 September 2009

Abstract
Purpose *N*-[2-(Dimethylamino)ethyl]-2,6-dimethyl-1-oxo-1, 2-dihydrobenzo[b]-1,6-naphthyridine-4-carboxamide (SN 28049) is a potent DNA binding topoisomerase II poison that shows excellent antitumour activity in a colon-38 murine tumour model in comparison to standard topoisomerase II poisons. We report here the preclinical pharmacokinetics of SN 28049.
Methods C57 Bl/6 mice ($n = 3$ per time point) were treated with a single i.v., i.p. or p.o. administration (8.9 mg/kg). Plasma and tissue samples were analysed using a validated LC/MS method utilizing a homologue as an internal standard.
Results The assay range was 0.062–2.5 μM with a quantitation limit of 0.062 μM and a detection limit of 0.025 μM. Acceptable intra- and inter-assay accuracy (95–105%) and precision (<6.5% RSD) were achieved. Following i.v. administration, SN 28049 demonstrated 2-compartment model kinetics with a volume of distribution of 42.3 ± 4.1 l/kg, a plasma clearance of 12.1 ± 0.5 l/h per kg and distribution and elimination half-lives of 0.15 ± 0.02 and 2.8 ± 0.2 h (mean ± SE), respectively. For all administration routes, SN 28049 concentrations in normal tissues (brain, heart, liver, lung, and kidney) were 12- to 120-fold higher than those in plasma, but half-lives and mean residence times were similar. The i.p. and p.o. bioavailabilities were 83.1 ± 1.5 and 54.5 ± 1.1%, respectively. In the tumour tissue, elimination half-life (9.1 ± 0.7 h) and the mean residence time (18.2 ± 0.7 h) were significantly ($P < 0.001$) longer than those of plasma and normal tissues. The tumour area under the concentration–time curve (AUC) (1,316 ± 66 μM h) was also 693-fold greater than the plasma AUC, and considerably higher (~5-fold) than any other tissue examined, indicating selective uptake and retention of SN 28049 in the tumour.
Conclusion We conclude that SN 28049's high tumour exposure and long tumour retention time is likely to contribute to its high antitumour activity in vivo.

Keywords SN 28049 · Benzonaphthyridine · LC–MS · Pharmacokinetics · Cancer · Topoisomerase poison

P. B. Lukka · P. Kestell · B. C. Baguley (✉)
Auckland Cancer Society Research Centre,
Faculty of Medical and Health Sciences,
The University of Auckland, Private Bag 92019,
Auckland, New Zealand
e-mail: b.baguley@auckland.ac.nz

P. B. Lukka · J. W. Paxton
Department of Pharmacology and Clinical Pharmacology,
Faculty of Medical and Health Sciences,
The University of Auckland, Private Bag 92019,
Auckland, New Zealand

Introduction

DNA intercalating anticancer agents such as amsacrine, actinomycin D, daunorubicin and doxorubicin have had a long history in cancer chemotherapy [1, 2]. Further acridine derivatives asulacrine and *N*-[2-(dimethylamino)ethyl]acridine-4-carboxamide (DACA) were developed during a drug discovery programme in this laboratory with the aim of identifying anticancer agents that had a broader spectrum of clinical activity [3, 4]. DACA was not only highly active against an experimental solid tumour but was also able to overcome resistance in vitro using cell lines that over expressed either P-glycoprotein or multidrug protein resistance (MRP) [5]. It was advanced to clinical trial [6–9] but further clinical development was prevented by a

side effect involving a burning sensation near the site of administration. A search for analogues that might overcome this side effect led to the identification of the DNA binding benzonaphthyridine, *N*-[2-(dimethylamino)ethyl]-2,6-dimethyl-1-oxo-1,2-dihydrobenzo[b]-1,6-naphthyridine-4-carboxamide (SN 28049), which was found to have much greater dose potency than DACA [10]. SN 28049, in contrast to DACA, was able to induce complete regression in vivo of subcutaneous implants of the murine colon-38 adenocarcinoma, a tumour relatively resistant to topoisomerase II poisons such as amsacrine, doxorubicin and etoposide using doses that were 20-fold lower than that of DACA. The in vitro cytotoxicity of SN 28049 was approximately 50-fold more potent than DACA [11]. We wished to establish whether pharmacokinetics played a role in the superior antitumour properties of this agent, and we have therefore determined the tissue and plasma pharmacokinetics in both non-tumour-bearing and colon-38 tumour-bearing mice using i.v., i.p., and p.o. routes of administration.

Materials and methods

Materials

SN 28049 (Fig. 1a) (free base, 99% pure by LC; MW, 338) and the internal standard (IS) SN 28507 (Fig. 1b) (free base, 98% pure by LC; MW, 324) were synthesized in the Auckland Cancer Society Research Centre by Graham Atwell. Unless otherwise stated, all other chemicals were commercially available and of analytical grade. Ethylene disodium tetra acetic acid (EDTA) anticoagulant from Bio Chemed (Winchester, VA, USA) was used for preparation of plasma. Water used in all experiments was purified by filtering through ion exchange columns and a 0.22 μ filter (Milli-Q purification system, Millipore Corporation, Bedford, USA).

Mice

C57 Bl/6 female and male mice (20–25 g, 8–12 weeks old) were housed under constant temperature, humidity and lighting (12 h light per day). All experiments which included blood collection in mice from the ocular sinus under isofluorane anaesthesia were approved by The University of Auckland Animal Ethics Committee, and conformed to the Guidelines for the Welfare of Animals in Experimental Neoplasia, as set out by the United Kingdom Co-ordinating Committee on Cancer Research.

Methods

Drug formulation and administration

SN 28049 (free base) was dissolved in phosphate buffered saline (PBS) (890 µg/ml) and administered to mice at a dose of 8.9 mg/kg (26.3 µmol/kg) (a volume of 10 µl/g). This dose was chosen as it was the single optimal dose for the cure of colon-38 adenocarcinoma subcutaneously implanted in C57 Bl/6 female mice [12]. I.p. administration was carried out by injecting the drug into the peritoneal cavity using a 1 cc/ml Tuberculin syringe (Terumo, Laguna, Philippines) with a 26 gauge needle. Oral (p.o.) administration was achieved using a 3.8 cm curved stainless steel 20 gauge gavage needle (Harvard apparatus, Holliston, MA, USA); while the intravenous (i.v.) bolus injection (10 µl/g body weight) was via the tail vein using a 1 cc/ml Tuberculin syringe with a 27 gauge needle.

Tumour implantation and processing

The murine colon-38 adenocarcinoma is an in vivo transplantable tumour rather than a tumour cell line, and was originally obtained from the Mason Research Institute (Worcester, MA, USA). Tumours were maintained by serial passage in C57 Bl/6 mice and grown to approximately 9 mm in diameter before passaging. Donor mice were killed by cervical dislocation and tumours were removed and transferred to a Petri dish (Falcon Labware, Becton Dickson and Co., Franklin Lakes, NJ, USA) containing 10 ml PBS. Tumour fragments (1 mm^3) were implanted subcutaneously into recipient mice previously anaesthetized by i.p. administration (10 µl/g body weight) of a xylazine (10 mg/kg)/ketamine (150 mg/kg) mixture. The incision was closed using a Michel wound clip (Aesculap, Tuttlingen, Germany). Experiments were carried out in

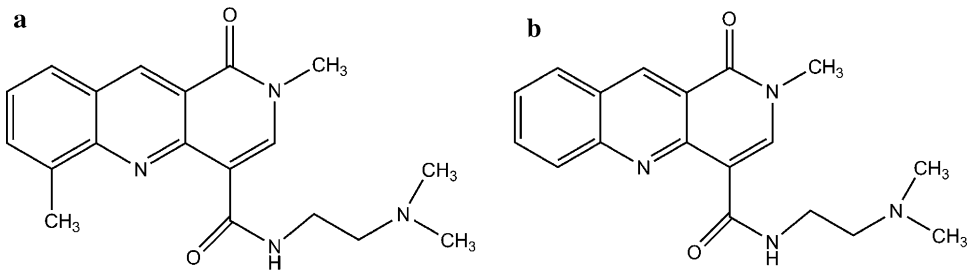

Fig. 1 **a** Chemical structure of SN 28049 and **b** SN 28507 (IS)

recipient mice when tumours were approximately 9 mm in diameter, 15–20 days after implantation.

Pharmacokinetic study design

Non-tumour-bearing male mice were used for the i.v., i.p., and p.o. pharmacokinetic and tissue distribution studies. Mice ($n = 3$) were administered 8.9 mg/kg of SN 28049 via each route. Blood and tissue samples were collected at various time points (0.08, 0.5, 1, 2, 4, 8, 12, and 24 h). Female tumour-bearing mice ($n = 3$) were used to study the pharmacokinetics and distribution in the tumour after i.p. injection. Blood and tumour samples were collected at various time points up to 72 h (0.08, 0.5, 1, 2, 4, 8, 12, 24, 48 and 72 h).

Preparation of mouse plasma and tissue homogenates

Mouse plasma was prepared from blood of anaesthetized C57 Bl/6 mice and stored at −80°C. To prevent coagulation, blood was collected in 1.5 ml microfuge tubes containing 20 µl of 7.5% EDTA and the plasma separated from red blood cells by centrifugation at 5,000*g* for 10 min. Tissues (brain, heart, kidney, liver, lung, and tumour) were collected after cervical dislocation of the anaesthetized mice. Collected tissues were washed with 1 ml PBS to remove blood contamination, briefly dried, transferred to 1.5 ml microfuge tubes and stored at −80°C. Frozen tissues were thawed at room temperature (25°C) and transferred in to glass tubes, weighed and homogenized in PBS (4-volumes) using a tissue homogenizer (S/N TH-71, Omni TH homogenizer, Gainesville, VA, USA) operated at 24,000 rpm.

Sample preparation

Triplicates of calibrants (drug added to mouse plasma and tissue homogenate at known concentrations) and pharmacokinetic samples were added to 12 × 75 mm glass tubes followed by 100 µl of IS (0.2 µM). The sample was then deproteinized by addition of ten volumes of 3:1 ice cold MeCN:MeOH, and thoroughly mixed for 30 s using a vortex mixer. After centrifugation (3,000*g* at 4°C) for 15 min, the clear supernatants were transferred to 12 × 75 mm glass tubes and concentrated in a centrifugal vacuum concentrator. The concentrated extract was then reconstituted in 100 µl of mobile phase and injected (5 µl) in to the Liquid Chromatograph-Mass Spectrometer (Agilent®, Avondale, PA) (LC/MS) for analysis.

LC/MS method and analysis

An Agilent® 1100 series capillary LC system was used with a capillary pump, an auto sampler, and an ion trap mass spectrometer (Agilent®, Avondale, PA, USA). System control and data acquisition were carried out with the Agilent LC-MSD trap software ver. 5.3, incorporating the MSD Trap Control software from Bruker Daltonics (Fahrenheitstr, Bremen, Germany). An Agilent Zorbax C18 5 μ (150 × 0.5 mm) column pre-equilibrated for 30 min at 20 µl/min was used to achieve chromatographic separation of the analytes. Isocratic elution with 20% MeCN, 79.9% Milli Q water, 0.1% formic acid and 5 mM ammonium formate was employed with the first 2 min of the run diverted to waste. The elution time was 9 min for SN 28049 and 4.5 min for the IS. A post-run equilibration of 3 min was used to remove any interference for the subsequent run. The MS2 fragments of SN 28049 [M+H]+ (*m*/*z* 339^294) and IS [M+H]+ (*m*/*z* 325^280) were selectively monitored using the ion trap mass spectrometer with the following conditions: fragmentation amplitude, 1.0 V; interface, electrospray; mode of ionization, positive; drying gas (nitrogen), 5 l/min; nebulizer pressure, 10 psi; drying temperature, 250°C; capillary voltage, 40.5 V; skimmer voltage, 45.66 V; capillary exit, 172.95 V; ion charge control target, 20,000; maximum accumulation time, 20 ms; scan range, 200–400 *m*/*z*; scan mode, standard + enhanced; scan speed, 13,000 *m*/*z* per s.

Plasma and tissue samples were analysed by a previously published method [13]. The assay range was 0.062–2.5 µM with a quantitation limit of 0.062 µM and a detection limit of 0.025 µM. Acceptable intra- and inter-assay precision (<12.8% RSD) and accuracy (92–103%) were achieved in all tissues. The absolute recoveries of SN 24089 (0.062–1.0 µM) and the IS (0.2 µM) were found to be >81.1 ± 3.1 and >83.5 ± 1.5%, respectively.

Pharmacokinetic and statistical analysis

The area under the plasma concentration–time curve (AUC) was computed by the log-trapezoidal rule, extrapolated to infinity by addition of the value Ct/β, where Ct is the concentration at the last time point, and β is the terminal slope determined by log-linear regression. The elimination half-life ($T_{1/2\beta}$) was calculated by the equation ln2/β. The terms C_{max} and T_{max} represent the maximum concentration achieved and the time to maximum concentration respectively, and were determined from the concentration–time profiles. The bioavailability (F) was calculated as the ratio of the AUC after i.p. and p.o. dosing to the AUC after i.v. dose (all at the same dose, 8.9 mg/kg). The model-independent pharmacokinetic parameters, clearance (CL), volume of distribution at steady state (V_{ss}), and mean residence time (MRT) were calculated by the following equations: CL = F × dose/AUC; $V_{ss} = (F \times \text{Dose} \times \text{AUMC})/(\text{AUC})^2$, and MRT = AUMC/AUC; where AUMC represents the total area under the first moment of the concentration–time curve, computed in a similar fashion to that used for AUC.

The plasma concentration–time profiles were fitted to various models (one vs. two-compartment, with first-order or zero-order inputs for i.p. and p.o. administration). The Nedler-mead minimization process with 500 iterations was used with a weighting of $1/y^2$ for modelling the concentration–time data. The best-fit two-compartment model after i.v. administration was used as the basis for the i.p. and p.o. analysis, enabling an absorption half-life to be estimated for each route. WinNonlin® ver 5.0 (Pharsight® Corporation, Mountain view, CA, USA) was used for the model fitting and calculation of all pharmacokinetic parameters. The statistical differences between the groups were calculated using either student *t* test or one way ANOVA by SigmaStat® 3.5. In all analysis, a P value <0.05 was considered statistically significant.

Results

Plasma pharmacokinetics and bioavailability

Mean plasma concentrations and best-fit concentration–time profiles after i.v., i.p., and p.o. administration are shown in Fig. 2. The biphasic concentration–time elimination profile observed in plasma after an i.v. bolus dose indicated that a two-compartment model (with $T_{1/2\alpha}$—0.15 ± 0.02 and $T_{1/2\beta}$—2.8 ± 0.2 h) was the most appropriate pharmacokinetic model to describe SN 28049 concentrations in mice. This two-compartment model was used as the basic model to fit the other i.p. and p.o. routes with either first-order or zero-order input. The best-fit for both routes was given with a first-order input with absorption half-lives of 0.1 ± 0.02 and 0.26 ± 0.01 h after i.p. and p.o., respectively. The volume of distribution in the central compartment (V_c) was 42.3 ± 4.1 l/kg (i.v.), 41.0 ± 5.0 l/kg (i.p.) and 38.1 ± 3.0 l/kg (p.o.). Pharmacokinetic parameters for these models and also from model-independent analysis of the plasma concentration–time data are reported in Table 1. Comparison of AUCs after i.p. and p.o. administration with i.v., gave bioavailabilities of 83.1 ± 1.5 and 54.5 ± 1.1%, respectively. The rate of entry of SN 28049 into the systemic circulation was considerably slower after p.o. than i.p., with a lower C_{max} (0.2 ± 0.01 vs. 0.6 ± 0.07 μM) and a longer T_{max} (2.0 vs. 0.5 h). The elimination $T_{1/2\beta}$ (4.1 ± 0.1 h) after p.o. was slightly longer than that after i.p. (2.5 ± 0.2 h) and i.v. (2.8 ± 0.2 h) was statistically significant ($P = 0.001$). Total plasma clearances (CL) by all routes were not significantly different (i.v.—12.1 ± 0.5; i.p.—12.1 ± 0.3; and p.o.—12.0 ± 0.6 l/h per kg). There were no significant differences between the major plasma pharmacokinetic parameters (CL, V_{ss}, $T_{1/2\beta}$ and AUC) after i.p. administration in tumour bearing (Table 3) compared to healthy mice (Table 1).

Tissue distribution

Following i.v. administration, SN 28049 was rapidly distributed into tissues and reached the C_{max} within 5 min (T_{max}).

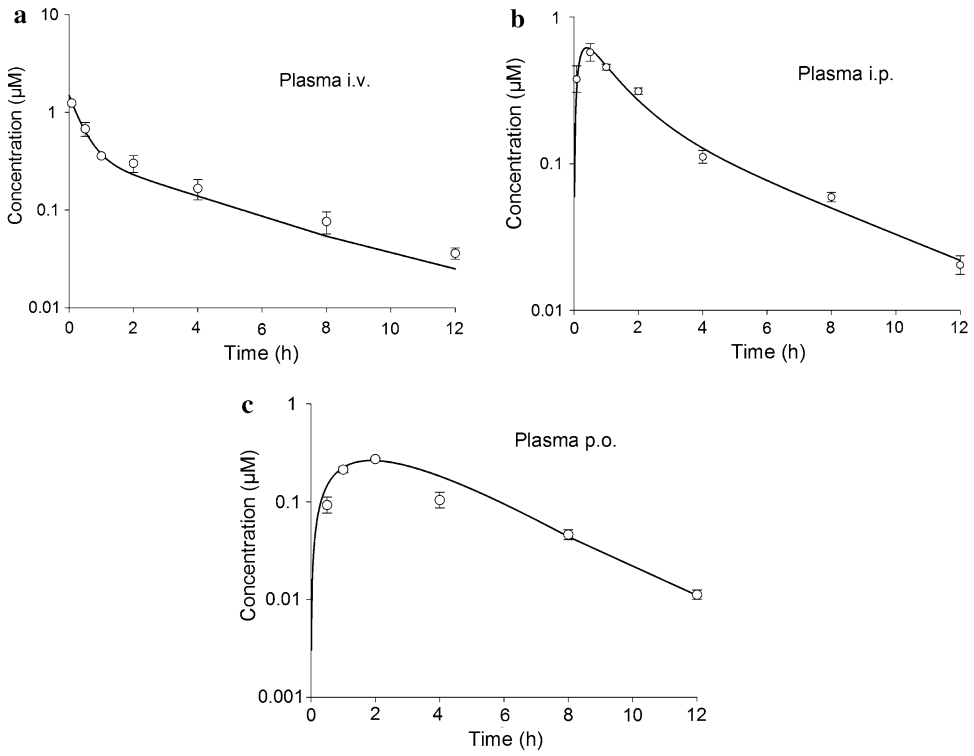

Fig. 2 Two-compartment model fit for plasma concentration–time data after **a** i.v., **b** i.p., and **c** p.o. administration of SN 28049 in C57 Bl/6 male mice. Each point represents the mean ± SE

Table 1 Plasma pharmacokinetic parameters after i.v., i.p., and p.o. administration of SN 28049 (8.9 mg/kg/26.3 μmol/kg) in C57 Bl/6 mice (n = 3 mice per time point)

Matrix	Non-compartmental analysis						Two-compartment model			
	AUC (μM h)	$T_{1/2\beta}$ (h)	CL (l/h/kg)	V_{ss} (l/kg)	T_{max} (h)	C_{max} (μM)	$T_{1/2\alpha}$ (h)	$T_{1/2\beta}$ (h)	CL (l/h/kg)	V_c (l/kg)
Plasma i.v.	2.2 ± 0.1	2.3 ± 0.2	12.0 ± 0.5	34.6 ± 2.2	0.08	1.2 ± 0.05	0.15 ± 0.02	2.8 ± 0.2	12.1 ± 0.5	42.3 ± 4.1
Plasma i.p.	1.8 ± 0.1	2.5 ± 0.2	12.1 ± 0.3	41.2 ± 2.4	0.5	0.6 ± 0.07	0.1 ± 0.02[a]	2.7 ± 0.2	13.0 ± 0.3	41.0 ± 5.0
Plasma p.o.	1.2 ± 0.07	4.1 ± 0.1	12.1 ± 0.6	43.5 ± 3.5	2.0	0.2 ± 0.01	0.26 ± 0.01[a]	3.4 ± 0.1	11.1 ± 0.2	38.1 ± 3.0

Values are represented as mean ± SE

[a] Absorption half-life

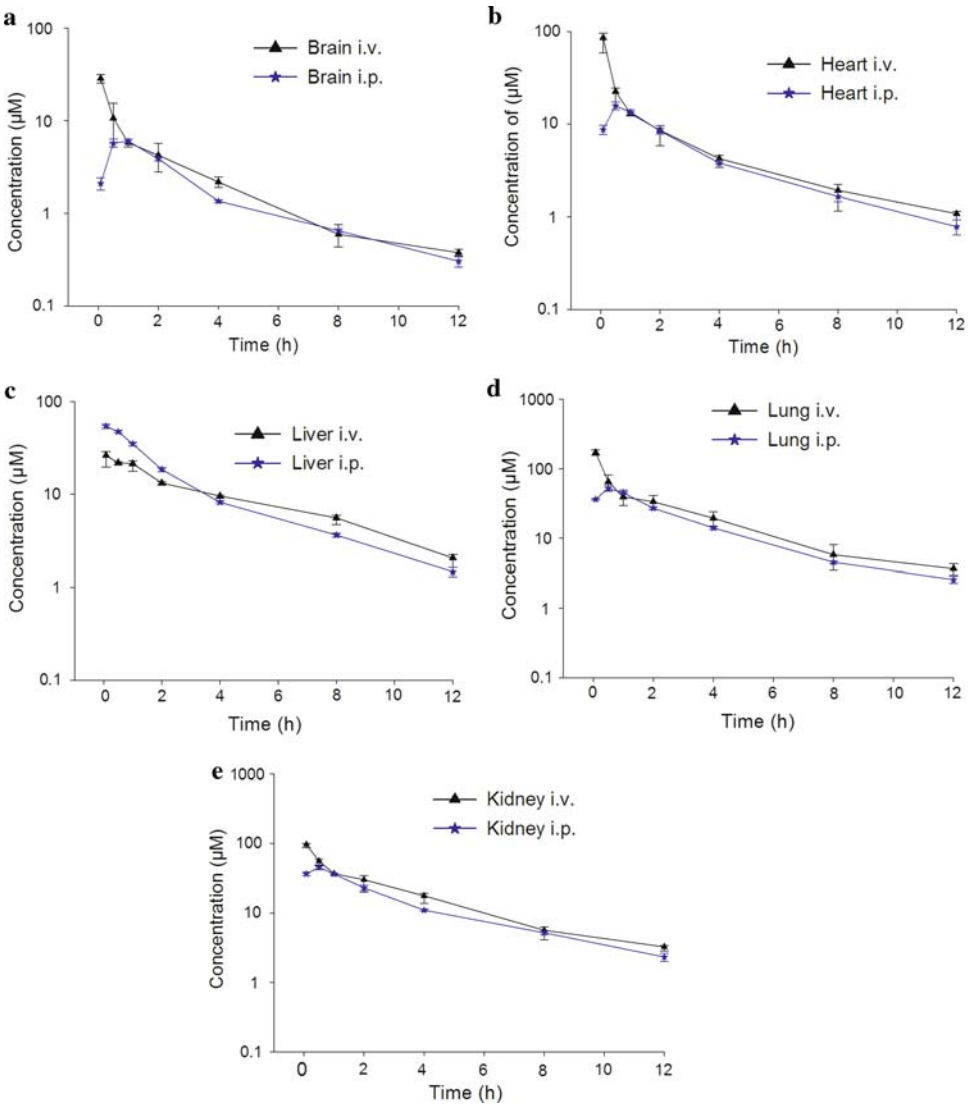

Fig. 3 Concentration–time profiles in tissues obtained in **a** brain, **b** heart, **c** liver, **d** lung, **e** kidney from C57 Bl/6 male mice (n = 3) after i.v. and i.p. administration of SN 28049 (8.9 mg/kg). Each point represents the mean ± SE

The highest tissue concentrations were observed in lung, followed by kidney, liver, heart and brain, and were 10- to 100-fold greater than the equivalent plasma concentrations (Fig. 3). Similarly the tissue/plasma AUC ratios were of the same order of magnitude with values that ranged from 120 for lung to 17 for brain (Table 2). The terminal half-life ($T_{1/2\beta}$) of SN 28049 was greatest in liver (3.7 ± 0.3 h), while in plasma and the other tissues examined, it ranged between 2.0 and 2.8 h (SE ± 0.2). Mean residence time (MRT) was also greatest in the liver (5.3 ± 0.5 h). Of all the tissues examined, the brain appeared to have the lowest exposure to SN 28049 after a single i.v. dose.

Table 2 Pharmacokinetic (non-compartmental analysis) parameters in tissues after i.v. and i.p. administration of SN 28049 (8.9 mg/kg/26.3 μmol/kg) in C57 Bl/6 male mice ($n = 3$ mice per time point)

Matrix	AUC (μM h)	C_{max} (μM)	T_{max} (h)	$T_{1/2\beta}$ (h)	Mean residence time (h)
Brain i.v.	33.8 ± 2.3 (16.8)	28.5 ± 1.4 (23.7)	0.08	2.2 ± 0.2	2.3 ± 0.2
Brain i.p.	21.0 ± 0.8 (11.6)	6.2 ± 0.5 (10.3)	0.5	2.2 ± 0.1	3.2 ± 0.2
Heart i.v.	83.3 ± 6.3 (41.6)	85.4 ± 5.9 (71.2)	0.08	2.8 ± 0.1	2.6 ± 0.3
Heart i.p.	52.6 ± 4.2 (29.2)	15.8 ± 2.3 (26.3)	0.5	2.3 ± 0.1	3.3 ± 0.3
Liver i.v.	109.3 ± 4.7 (54.5)	26.5 ± 3.8 (22.1)	0.08	3.7 ± 0.3	5.3 ± 0.5
Liver i.p.	173.5 ± 2.8 (96.4)	54.2 ± 4.9 (90.3)	0.08	2.3 ± 0.1	3.1 ± 0.2
Lung i.v.	240.7 ± 6.7 (120.0)	170.5 ± 0.6 (142.1)	0.08	2.0 ± 0.1	2.5 ± 0.1
Lung i.p.	158.4 ± 2.3 (88.1)	54.3 ± 5.4 (90.5)	0.5	2.3 ± 0.1	3.1 ± 0.1
Kidney i.v.	197.4 ± 7.7 (98.8)	96 ± 6.0 (80.1)	0.08	2.7 ± 0.2	3.3 ± 0.3
Kidney i.p.	153.7 ± 0.6 (85.5)	45.4 ± 5.3 (75.6)	0.5	2.9 ± 0.3	3.8 ± 0.4

Values are represented as mean ± SE. The tissue to plasma ratios of AUC and C_{max} are indicated in the parentheses

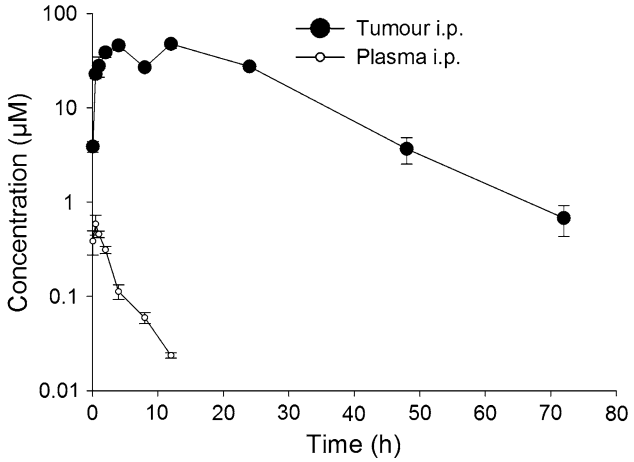

Fig. 4 Concentration–time profiles in plasma and tumour obtained from C57 Bl/6 female mice ($n = 3$) after i.p. administration of SN 28049 (8.9 mg/kg). Each point represents the mean ± SE

On i.p. administration, distribution from the intraperitoneal cavity to the plasma and tissues was relatively rapid with C_{max} observed after 30 min (except for liver, where the maximal concentrations were reached at 5 min). The ratios of tissue to plasma AUC were of similar magnitude as for i.v. administration with values ranging from 96 for liver to 11 for brain. Following oral administration, concentrations in liver were almost 100-fold higher than plasma and similar in magnitude to those observed in liver after i.v. and i.p. administration.

Tumour distribution

Concentration–time profiles in plasma and tumour tissue following i.p. administration of SN 28049 (8.9 mg/kg) to tumour-bearing female mice (C57 Bl/6) are shown in Fig. 4 and pharmacokinetic parameters are reported in Table 3. SN 28049 was taken up and retained by tumour tissue as demonstrated by the high AUC (1,316 ± 66 μM h). The tumour tissue to plasma ratio (692) was considerably higher than that previously observed for the healthy tissues. The distribution to the tumour tissue was slow and variable with a C_{max} (48.1 ± 3.0 μM) at approximately 6–12 h. Tumour $T_{1/2\beta}$ (9.1 ± 0.7 h) and MRT (18.2 ± 0.2 h) were prolonged and significantly greater ($P < 0.001$) than that observed in plasma and other tissues.

Discussion

Plasma pharmacokinetics, bioavailability, tumour and tissue distribution of SN 28049 have been assessed after i.v., i.p., and p.o administration to mice. No significant difference was observed with CL ($P = 0.98$) and V_{SS} ($P = 0.083$) calculated using the non-compartmental and two-compartment analysis. SN 28049 had a high volume of distribution with no significant differences ($P = 0.56$) among the various administration routes. However, SN 28049 had a slower rate of absorption following p.o. administration than following i.p. administration. Distribution to tissues (brain, heart, liver, lung and kidney) was rapid and tissue concentrations were 12- to 120-fold higher than those in plasma. Following i.p. administration, the highest concentrations of SN 28049 (AUC) were observed in the liver, suggesting rapid absorption of SN 28049 from the peritoneal cavity into the liver.

A different profile was observed in tumour tissue. The tumour concentrations reached a maximum after 6–12 h, which was longer than that in normal tissues ($T_{max} \leq 2$ h). The $T_{1/2\beta}$ and MRT were also significantly longer ($P < 0.001$) compared to plasma and other tissues, and SN 28049 was measurable in tumour for up to 72 h following a single i.p. dose, at which time the concentrations in plasma and other tissue were below the limit of detection. This

Table 3 Plasma and tumour pharmacokinetic parameters after i.p. administration of SN 28049 (8.9 mg/kg/26.3 μmol/kg) in C57 Bl/6 female tumour-bearing mice ($n = 3$ mice per time point)

Matrix	AUC (μM h)	C_{max} (μM)	T_{max} (h)	$T_{1/2\beta}$ (h)	Mean residence time (h)	CL (l/h/kg)	V_{SS} (l/kg)
Plasma	1.9 ± 0.1	0.8 ± 0.01	0.08	2.7 ± 0.1	3.2 ± 0.2	12.6 ± 0.4	41.9 ± 3.3
Tumour	1316 ± 66 (692.6)	48.1 ± 3.0(60.1)	12	9.1 ± 0.7	18.2 ± 0.1	–	–

Values are represented as mean ± SE. The tissue to plasma ratios of AUC and C_{max} are indicated in the parentheses

Table 4 Comparison of tumour and plasma pharmacokinetic parameters (at curative doses) of SN 28049 (8.9 mg/kg/26.3 μmol/kg), DACA (150 mg/kg/511 μmol/kg) and doxorubicin (10 mg/kg/18.4 μmol/kg) in C57 Bl/6 female tumour-bearing mice ($n = 3$ mice per time point) for SN 28049 and BDF_1 mice for DACA and doxorubicin

Tumour			Plasma			
Drug	AUC (μM h)	$T_{1/2\beta}$ (h)	AUC (μM h)	$T_{1/2\beta}$ (h)	CL (l/h/kg)	V_{SS} (l/kg)
SN 28049	1316 ± 66	9.1 ± 0.7	1.9 ± 0.1	2.7 ± 0.1	12.6 ± 0.4	41.9 ± 3.3
DACA	431 ± 10	16.3	23.4 ± 0.1	2.7 ± 0.3	17.5 ± 0.2	11.8 ± 1.4
Doxorubicin	239 ± 0.1	45	1.46 ± 0.1	10.6 ± 0.1	150.3 ± 0.1	2009.0

slow uptake into the tumour, as well as the slow elimination, might be due partly to the low vascular density and correspondingly longer drug diffusion distances of tumour tissue as compared to normal tissues such as heart, liver, kidney. It may also be a consequence of high DNA binding within tumour tissue; the binding constant of SN 28049 for the DNA copolymer poly (dG–dC)·poly (dG–dC) is approximately 7-fold higher than that for DACA and 15-fold higher than that for amsacrine (Baguley, B.C., unpublished data). High DNA binding leads to lower free drug concentrations and consequently to lower rates of drug diffusion.

Comparison of the tumour pharmacokinetics of SN 28049 with that of doxorubicin [14] and DACA [15] in the colon-38 mouse tumour model at maximum tolerated doses indicated a more efficient distribution from plasma to tumour tissue for SN 28049 (Table 4). Although the tumour tissue elimination half-life for doxorubicin (45 h) was longer than that for DACA (16 h) and SN 28049 (9 h), the absolute tumour exposure, as measured by the AUC, was greatest for SN 28049 (1,316 μM h) compared to DACA (431 μM h) and doxorubicin (239 μM h). The tumour/plasma AUC ratio was also greatest for SN 28049 (693) compared to doxorubicin (164) and DACA (18.4). Comparative values for amsacrine and asulacrine in colon-38 tumour tissue are not available, but in Lewis lung tumour tissue, the corresponding AUC ratios were 6.2 for amsacrine and 2.2 for asulacrine [16]. It is worth noting that the terminal half-life of doxorubicin in heart tissue (58 h), which has been suggested to be a cause of its cardiotoxicity [14], is much longer than that for SN 28049 (2.3–2.8 h; Table 2).

In conclusion, this study demonstrates that SN 28049 exhibits greater selective uptake and retention in tumour tissue compared to that observed with a number of other DNA intercalating drugs such as doxorubicin, amsacrine, asulacrine and DACA. It appears highly likely that this will play a part in determining the superior in vivo antitumour activity of SN 28049 in colon-38 tumour bearing mice. We are currently investigating analogues of SN 28049 to determine which structural features and physicochemical properties may play a part in determining its superior tumour pharmacokinetic properties.

Acknowledgments This study was supported by the Auckland Cancer Society and Auckland Uniservices Ltd., New Zealand.

References

1. Dalgliesh CE, Todd AR (1949) Actinomycin. Nature 164:830
2. Blum RH, Carter SK (1974) Adriamycin. A new anticancer drug with significant clinical activity. Ann Intern Med 80:249–259
3. Baguley BC, Denny WA, Atwell GJ, Finlay GJ, Rewcastle GW, Twigden SJ, Wilson WR (1984) Synthesis, antitumour activity, and DNA binding properties of a new derivative of amsacrine, *N*-5-dimethyl-9-[(2-methoxy-4-methylsulfonylamino)-phenylamino]-4-acridinecarboxamide. Cancer Res 44:3245–3251
4. Atwell GJ, Rewcastle GW, Baguley BC, Denny WA (1987) Potential antitumour agents. 50. In vivo solid-tumor activity of derivatives of *N*-[2-(dimethylamino)ethyl]-acridine-4-carboxamide. J Med Chem 30:664–669
5. Davey RA, Su GM, Hargrave RM, Harvie RM, Baguley BC, Davey MW (1997) The potential of *N*-[2-(dimethylamino) ethyl]acridine-4-carboxamide] to circumvent three multidrug-resistance phenotypes in vitro. Cancer Chemother Pharmacol 39:424–430
6. McCrystal MR, Evans BD, Harvey VJ, Thompson PI, Porter DJ, Baguley BC (1999) Phase I study of the cytotoxic agent *N*-[2-(dimethylamino)ethyl]acridine-4-carboxamide. Cancer Chemother Pharmacol 44:39–44
7. Twelves C, Campone M, Coudert B, Van den Bent M, de Jonge M, Dittrich C, Rampling R, Sorio R, Lacombe D, de Balincourt C,

Fumoleau P (2002) Phase II study of XR5000 (DACA) administered as a 120-h infusion in patients with recurrent glioblastoma multiforme. Ann Oncol 13:777–780
8. Dittrich C, Coudert B, Paz-Ares L, Caponigro F, Salzberg M, Gamucci T, Paoletti X, Hermans C, Lacombe D, Fumoleau P (2003) Phase II study of XR 5000 (DACA), an inhibitor of topoisomerase I and II, administered as a 120-h infusion in patients with non-small cell lung cancer. Eur J Cancer 39:330–334
9. Caponigro F, Dittrich C, Sorensen JB, Schellens JH, Duffaud F, Paz Ares L, Lacombe D, de Balincourt C, Fumoleau P (2002) Phase II study of XR 5000, an inhibitor of topoisomerases I and II, in advanced colorectal cancer. Eur J Cancer 38:70–74
10. Deady LW, Rodemann T, Zhuang L, Baguley BC, Denny WA (2003) Synthesis and cytotoxic activity of carboxamide derivatives of Benzo[b] [1, 6]naphthyridines. J Med Chem 46:1049–1054
11. Bridewell D, Porter A, Finlay G, Baguley B (2008) The role of topoisomerases and RNA transcription in the action of the antitumour benzonaphthyridine derivative SN 28049. Cancer Chemother Pharmacol 62:753–762
12. Deady LW, Rogers ML, Zhuang L, Baguley BC, Denny WA (2005) Synthesis and cytotoxic activity of carboxamide derivatives of benzo[b][1, 6]naphthyridin-(5H)ones. Bioorg Med Chem 13:1341–1355
13. Lukka PB, Kestell P, Paxton JW, Baguley BC (2008) Development, validation of a liquid chromatography-mass spectrometry (LC–MS) assay for the determination of the anti-cancer agent *N*-[2-(dimethylamino)ethyl]-2,6-dimethyl-1-oxo-1,2-dihydrobenzo[b]-1,6-naphthyridine-4-carboxamide (SN 28049). J Chromatogr B 875:368–372
14. Formelli F, Carsana R, Pollini C (1986) Comparative pharmacokinetics and metabolism of doxorubicin and 4-demethoxy-4′-O-methyldoxorubicin in tumor-bearing mice. Cancer Chemother Pharmacol 16:15–21
15. Paxton JW, Young D, Evans SMH, Robertson IGC, Kestell P (1993) Tumour profile of *N*-[2-(dimethylamino)ethyl]acridine-4-carboxamide after intraperitoneal administration in the mouse. Cancer Chemother Pharmacol 32:320–322
16. Kestell P, Paxton JW, Evans PC, Young D, Jurlina JL, Robertson IGC, Baguley BC (1989) Disposition of amsacrine and its analogue 9-([2-Methoxy-4-[(methylsulfonyl)-amino]phenyl]amino)-*N*,5-dimethyl-4-acridinecarboxamide (CI-921) in plasma, liver, and Lewis lung tumors in mice. Cancer Res 50:503–508